

Article

Activity of Platinum-Based Cathode Electrocatalysts in Oxygen Redaction for Proton-Exchange Membrane Fuel Cells: Influence of the Ionomer Content

Anastasia Alekseenko ¹, Sergey Belenov ^{1,*}, Dmitriy Mauer ¹, Elizaveta Moguchikh ¹, Irina Falina ², Julia Bayan ¹, Ilya Pankov ³, Danil Alekseenko ¹ and Vladimir Guterman ¹

¹ Chemistry Faculty, Southern Federal University, Rostov-on-Don 344090, Russia; aalekseenko@sfedu.ru (A.A.); dima333000@yandex.ru (D.M.); liza.moguchix@mail.ru (E.M.); bayan.yulia@yandex.ru (J.B.); dvalekseenko@sfedu.ru (D.A.); guter@sfedu.ru (V.G.)

² Physical Chemistry Department, Faculty of Chemistry and High Technologies, Kuban State University, Krasnodar 350040, Russia; irina_falina@mail.ru

³ Research Institute of Physical Organic Chemistry, Southern Federal University, 194/2 Stachki St., Rostov-on-Don 344090, Russia; ipankov@sfedu.ru

* Correspondence: sbelenov@sfedu.ru

Abstract: Studying the ORR activity of platinum-based electrocatalysts is an urgent task in the development of materials for proton-exchange membrane fuel cells. The catalytic ink composition and the formation technique of a thin layer at the RDE play a significant role in studying ORR activity. The use of a polymer ionomer in the catalytic ink provides viscosity as well as proton conductivity. Nafion is widely used as an ionomer for research both at the RDE and in the MEA. The search for ionomers is a priority task in the development of the MEA components to replace Nafion. The study also considers the possibility of using the LF4-SK polymer as an alternative ionomer. The comparative results on the composition and techniques of applying the catalytic layer using LF4-SK and Nafion ionomers are presented, and the influence of the catalytic ink composition on the electrochemical characteristics of commercial platinum–carbon catalysts and a highly efficient platinum catalyst based on an N-doped carbon support is assessed.

Keywords: platinum-based electrocatalyst; electrochemical activity; oxygen reduction reaction; catalytic ink; N-doped carbon; ionomer; Nafion; LF4-SK polymer; proton conductivity; proton-exchange membrane fuel cells



Citation: Alekseenko, A.; Belenov, S.; Mauer, D.; Moguchikh, E.; Falina, I.; Bayan, J.; Pankov, I.; Alekseenko, D.; Guterman, V. Activity of Platinum-Based Cathode Electrocatalysts in Oxygen Redaction for Proton-Exchange Membrane Fuel Cells: Influence of the Ionomer Content. *Inorganics* **2024**, *12*, 23. <https://doi.org/10.3390/inorganics12010023>

Academic Editor: Paolo Fornasiero

Received: 28 November 2023

Revised: 25 December 2023

Accepted: 28 December 2023

Published: 2 January 2024



Copyright: © 2024 by the authors. Licensee MDPI, Basel, Switzerland. This article is an open access article distributed under the terms and conditions of the Creative Commons Attribution (CC BY) license (<https://creativecommons.org/licenses/by/4.0/>).

1. Introduction

The implementation success of devices with energy units based on proton-exchange membrane fuel cells (PEMFCs) depends on the performance of each of the components of the fuel cell, i.e., catalytic layers, proton-conducting membrane, and gas diffusion layer (GDL) [1–3]. The catalytic layers containing platinum nanoparticles (NPs) on a carbon support as well as a proton-conducting ionomer are among the most essential parts that ensure the flow of cell reactions at the cathode and anode of the PEMFC membrane electrode assembly (MEA). The catalytic layers for PEMFCs are obtained by distributing the catalytic ink over the surface of the GDL or membrane. To form the catalytic layers, the catalytic ink is used, which is obtained by mixing and dispersing the catalyst, solvent, and ionomer in an ultrasonic bath [4,5]. This leads to the formation of a porous structure of the catalytic layer consisting of a carbon support with active metal NPs distributed over its surface and a thin film of an ionomer surrounding the platinum and carbon particles, the structure of which largely determines the parameters of PEMFC operation [4,5].

An integral part of the catalytic layer is an ionomer due to the fact that this critical component of the catalytic layer contributes to (i) an increase in proton conductivity from the active centers to the membrane, (ii) an increase in the area of the triple phase boundary,

(iii) the holding of catalyst particles together, and (iv) the preservation of the mechanical integrity of the catalytic layer during manufacture and operation [4–8]. Moreover, this component provides water and gas balance inside the catalytic layer. During operation at the PEMFC cathode, oxygen passes between the Pt/C agglomerates, followed by diffusion through the ionomer film into the agglomerate directly to the platinum active center. The low content of the ionomer results in low proton conductivity and, thus, an increase in the resistance of the catalytic layer [8,9]. A large amount of ionomer contributes to good proton conductivity inside the catalytic layer and at the same time blocks active sites of the catalyst, which makes them inaccessible to oxygen at the cathode and hydrogen at the anode [9,10].

The initial stage of evaluating the electrochemical characteristics of electrocatalysts is testing at the rotating disk electrode (RDE). At this stage, the influence of the ionomer turns out to be vital for measurement results. The oxygen reduction reaction (ORR) and the determination of the electrochemically active surface area (ESA) of the catalyst deposited onto the RDE are the principal ways to assess the electrochemical behavior of materials in laboratory conditions. The previous studies [8,11,12] show that the formation of a high-quality catalytic layer on the RDE surface is only possible with the selected composition and technique of application for each type of electrocatalyst.

During measurements without any ionomer, the Pt-based catalysts exhibit excellent activity in the ORR in a three-electrode cell [13–16]. According to the results of the analysis of recent publications, the Pt/C electrodes, the catalytic ink of which has been prepared without using the Nafion binding polymer, are established to exhibit specific and mass activity in the ORR ~1.8 times higher compared to the electrodes with a deposited catalytic layer, which includes Nafion. Therefore, it is shown that the actual ORR activity of electrocatalysts in perchloric acid is significantly higher when the ionomer is absent at the catalyst/acid interphase. Nevertheless, these measurements cannot be considered correct since, in the MEAs, the ionomer acts as an electrolyte and is located directly in the catalytic layers. It is also known that the absence of an ionomer when studying the catalysts on the RDE surface might lead to damage to the catalytic layer due to the detachment of catalyst particles. Therefore, to date, in most studies using the RDE, a Nafion-type ionomer is included in the composition of the catalytic layer, although its content may vary. Different studies propose changing the I:C ratio [11] from 0 [17] to 1.9 [18]. In [11], a methodological study of the effect of the Nafion/carbon ratio (I:C) in the range from 0 to 1.4 has been carried out, and it has been shown that this parameter does not affect the ESA value but has a substantial impact on the activity of the catalyst. The maximum activity is observed in the absence of Nafion; with an increase in the Nafion content, the activity decreases, and with the I:C ratio equal to 0.5, it goes to a constant level. Therefore, the authors recommend using this ratio [11]. According to the results of the study carried out, the authors recommend using the I:C ratio of 0.5 for the measurements at the RDE. In the study [19], the authors have used a different I:C ratio depending on the type of carbon support used. For instance, for the catalyst on the Vulcan XC-72 support, it is 0.125; this is 0.5 for the catalyst on the Ketjenblack support. Thus, the I:C ratio used varies significantly in different publications and may depend on the characteristics of the catalyst applied.

In numerous papers concerned with testing the catalysts in the MEAs, it is noted that there is an optimal amount of ionomer in the layer, which is a compromise between conductivity and mass transfer for the Pt/C catalysts. The I:C ratio is usually assumed to be 0.7 [4,20]. This value is deemed as a constant and usually does not change regardless of the composition of the prepared catalytic layer for the MEA of the fuel cell. On the other hand, a series of works note that the empirically determined optimal content of Nafion in the catalytic layer (30 wt.%) [21] is not universal for all types of catalysts and may depend on the type of carbon support used, the mass fraction of platinum in the catalyst, and its composition [22,23].

Currently, using the perfluorinated sulfonic acid (PFSA) polymers developed by DuPont (USA) in 1966 is mentioned widely [11,24,25] under the brand name Nafion. The

properties of all the newly obtained membrane materials of this type are compared with the properties of the Nafion membranes and ionomers, i.e., they may be deemed a particular reference. Recently, due to limited production and increased demand for this product, there has been a shortage of this component and some supply constraints in many countries. An urgent task in numerous studies is the selection of a monomer for the possibility of replacing the widespread Nafion while maintaining the higher characteristics of the catalytic layer that it provides.

Developments in the field of obtaining novel ion-exchange perfluorinated membranes are performed by various companies. Some of the widespread perfluorinated membranes have a similar structure (Acipex (Asahi Chemical Company, Osaka, Japan), Flemon (Asahi Glass Company, Osaka, Japan)) [26]. Dow offers membranes with a shorter side chain length compared to Nafion [27]. In Russia, the production of the equivalent membranes, which are called MF4-SK, and the ionomer, which is called LF4-SK, is launched in St. Petersburg by Plastpolymer JSC [28]. PFSA may differ in the number of fixed groups in macromolecules, which is reflected in the ion-exchange capacity or equivalent weight, as well as the length of the side chain (Aquivion and others). In this work, we used polymers that had an identical structural unit and differed only in the content of fixed groups. Therefore, the FTIR spectra for these polymers in a dry state are identical. The results obtained are general for polymers with a Nafion-type structure.

The hypothesis of this study implies that it is possible to use the LF4-SK ionomer, which is different from Nafion, for the catalytic ink of both the commercial platinum–carbon products and the new-type materials on a modified carbon support. The objects selected as electrocatalysts are of undoubted interest due to their high functional characteristics. We have sought to determine how, with standard equipment, it is possible to assess the quality of the layer on the RDE surface and its critical effect on the ORR activity of the electrocatalyst.

2. Results and Discussion

2.1. Study of the Catalysts Structure

The following dispersions of perfluorosulfonic acid have been used as binding components: 10% aqueous dispersion of Nafion DE-1020 (DuPont, USA) with an equivalent weight of 1000 g/mol (SO_3^-) and 10.2% isopropanol dispersion of LF-4SK (Plastpolymer JSC, Russia) with an equivalent weight of 980 g/mol (SO_3^-). The presented values of the equivalent weight indicate a slightly higher exchange capacity of the LF-4SK polymer. The composition of the dispersions exhibits the presence of both ionomers in proton form. The structural units of both the polymers are identical [29,30].

The commercial platinum–carbon materials with a 20% platinum loading have been selected as electrocatalysts for the preparation of the catalytic ink, including the commercial materials JM20 (HiSPEC3000, Johnson Matthey, UK) and PM20 (Prometheus R&D LLC, Russia), as well as the home-made material synthesized on an N-doped Pt/C support.

The X-ray diffraction (XRD) patterns (Figure 1) of all the platinum-based materials studied have a characteristic appearance [31]. The obtained X-ray diffraction patterns exhibit characteristic reflections of the carbon support C (002) in the region of values of about $25^\circ 2\theta$ and reflections of the metal phase of platinum with a face-centered cubic (FCC) lattice. The broadening of the metal phase reflections in the X-ray diffraction patterns for the Pt/C catalysts studied is associated with the smaller size of platinum crystallites, the size of which can be estimated by the Scherrer formula and is presented in Table 1. It is noteworthy that the Pt/C–N material is characterized by an extremely small crystallite size (amorphous), which can be estimated with a great error margin.

The considered platinum–carbon catalysts are characterized by different morphologies. The TEM micrographs of the JM20 catalyst (Figure 2e–g) exhibit the presence of agglomerates on the surface of the support with a diameter of 10–13 nm. There are no agglomerates present in the TEM micrographs of local sections of the PM20 (Figure 2a–c) and Pt/C–N (Figure 2i–k) samples. According to TEM, the PM20 and Pt/C–N electrocata-

lysts are characterized by the smallest average size of crystallites and NPs of about 2 nm (Table 1).

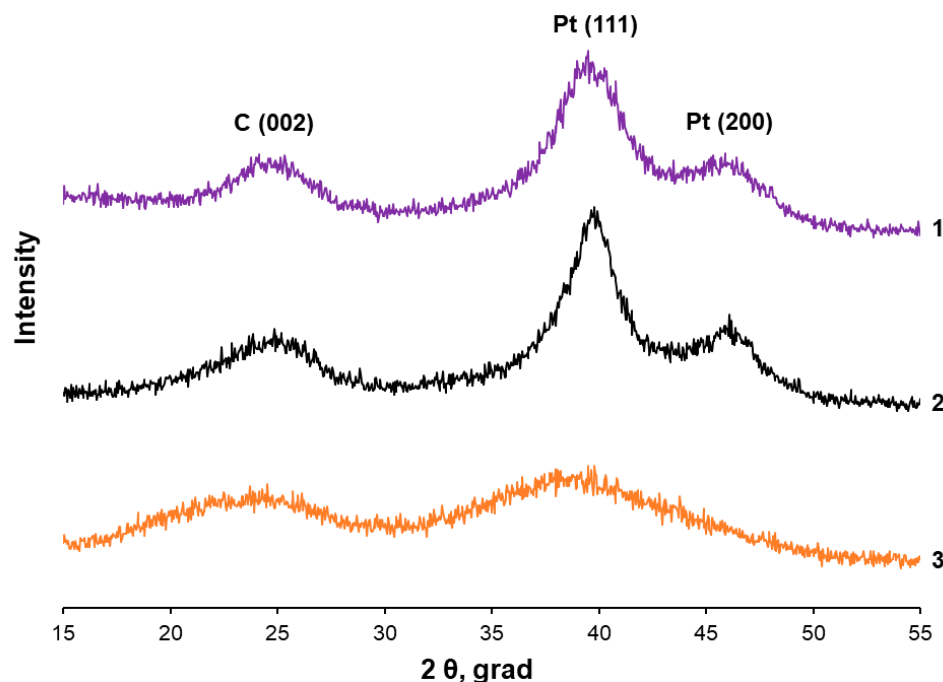


Figure 1. X-ray diffraction patterns of the Pt-based materials: 1—PM20, 2—JM20, 3—Pt/C–N.

Table 1. Composition, phase, and structure of the Pt-based materials.

Sample	Carbon Support	Pt Loading, %	D_{AV} , nm (XRD)	D_{NP} , nm (TEM)
JM20	Vulcan XC-72	20.0	2.5	2.7
PM20	Vulcan XC-72	20.0	2.0	2.0
Pt/C–N	Ketjenblack EC-300J	18.0	- *	2.3

* The crystallite size is difficult to calculate due to the pronounced broadening of the reflections. The presence of an X-ray amorphous phase is possible.

The TEM micrographs also exhibit a difference in the morphology of the carbon supports for the catalysts studied. For commercial PM20 and JM20, we can assume the use of the same Vulcan XC-72 support with a carbon sphere diameter of 30–60 nm. For the Pt/C–N electrocatalyst, the Ketjenblack EC-300J support has been used, which differs in morphology from the Vulcan XC-72 one.

To quantify the nature of the NPs' distribution over the surface of the carbon support using the TEM micrographs, an approach has been applied based on determining the proportion of NPs that have intersections with "neighboring" particles [32].

The PM20 and Pt/C–N materials are characterized by the presence of a higher proportion of individual NPs of more than 57% and 68%, respectively. Forty percent and thirty-nine percent, respectively, are the proportions of individual NPs and those that have intersections with one particle in JM20 (Figure 3b). The higher proportion of individual NPs for the Pt/C–N and PM20 materials characterizes a more uniform distribution of NPs over the support surface. Note that the positive effect of nitrogen heteroatoms on the uniformity of platinum NP deposition on carbon was previously observed in [33].

2.2. Features of the Formation of a Drop on the RDE Surface

During the course of the study and when optimizing the composition of the catalytic ink, a drop with a total volume of 8 μ L has been applied. The appearance of the drop has been recorded after each stage of the application, i.e., after applying 2 μ L (1 step), 3 μ L

(2 step), and 3 μL (3 step). Additionally, the effect of the RDE rotation during the drying of the catalytic ink on the RDE surface has been evaluated. For this purpose, the photofixation has been performed during the stationary drying and at the rotation completion at 700 rpm.

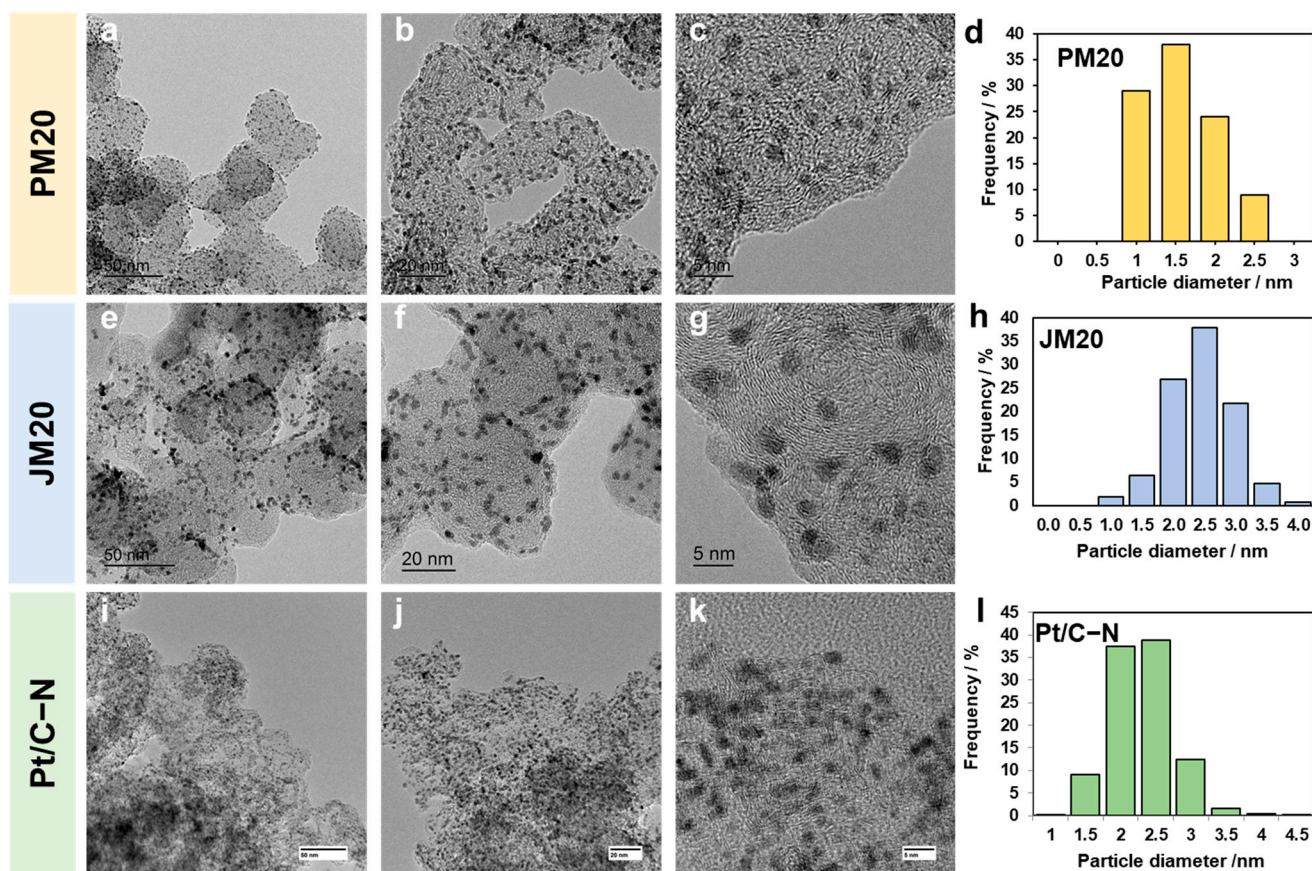


Figure 2. Micrographs of the PM20 (a–c), JM20 (e–g) and Pt/C–N (i–k) samples and histograms of the particles distribution in the samples: PM20 (d), JM20 (h) and Pt/C–N (l).

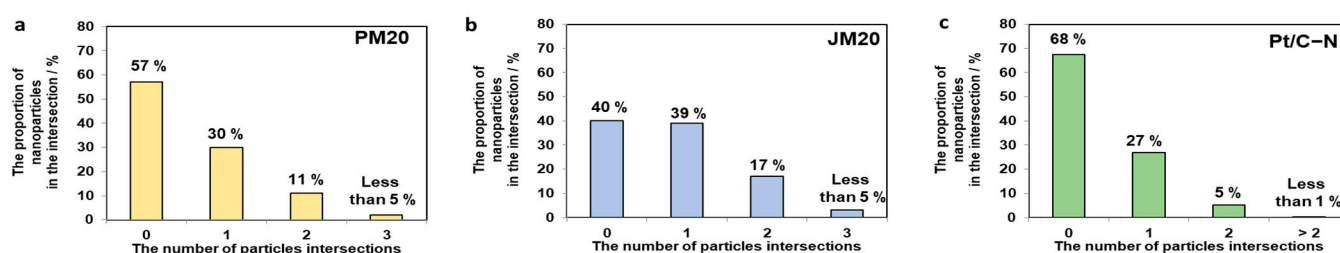


Figure 3. Intersection histograms: PM20 (a), JM20 (b), and Pt/C–N (c).

The ionomer acts as a binding component, without which the detachment of the catalytic layer from the surface of the RDE is quite possible, especially when studying the ORR activity at elevated rotation speeds of the disk electrode. However, at a higher concentration of the ionomer, the surface of platinum-based NPs may be blocked, which might result in an artificial underestimation of electrochemical characteristics. Therefore, at the first stage, an extended study of the effect of the amount of ionomer on the quality of the catalytic layer and, thus, the electrochemical characteristics of the JM20 electrocatalyst has been conducted by using the 1% Nafion solution and the 1%, 2%, and 0.05% LF4-SK solutions, respectively, as an ionomer. The use of the 1% Nafion solution as a monomer is a standard practice in the preparation of the catalytic ink in most of the scientific publications presented [5,22,34].

Based on the results of a visual inspection of the JM20 catalytic layer on the RDE surface, the following features can be noted. When the layer is formed sequentially in three stages by applying the 2, 3, and 3 μL drops of the ink onto the RDE, a more uniform coating is observed after the third stage. After the first and second drops, bare spots can be observed on the RDE surface (Figure 4e,p,q), as well as the partial formation of a layer with a so-called “coffee ring” (Figure 4b,g).

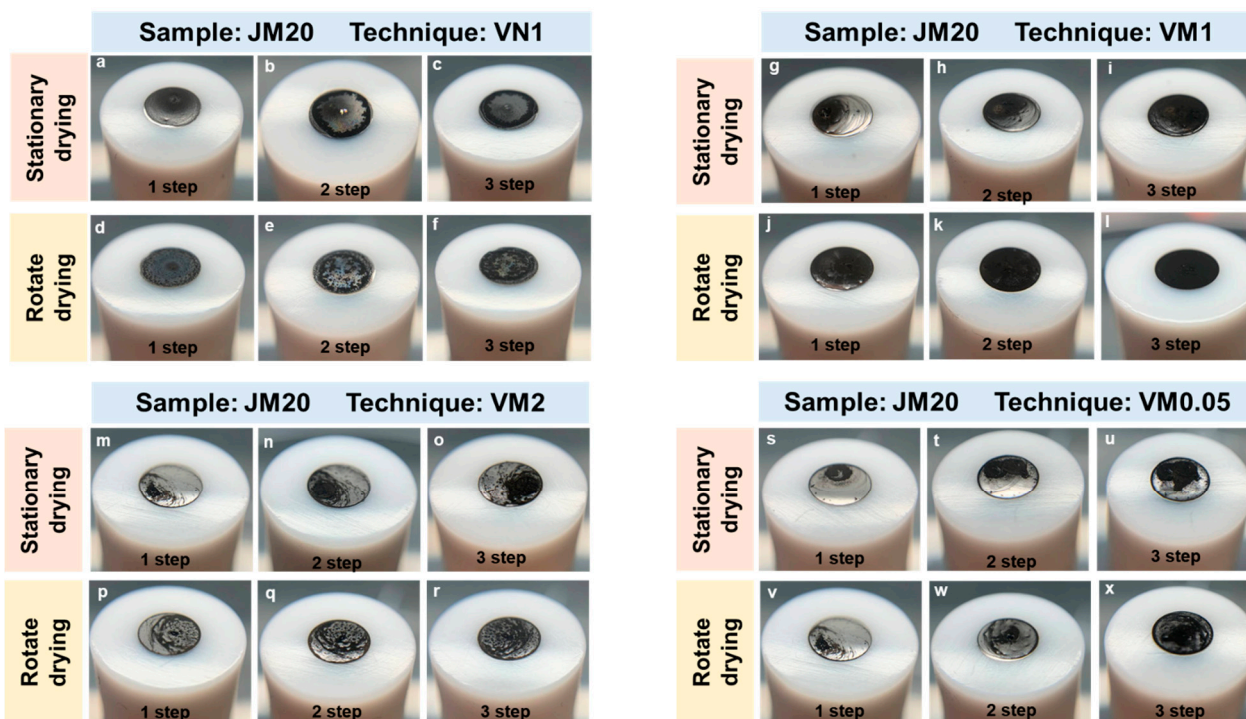


Figure 4. Photographs of the sequential formation of a thin layer at the RDE (after the 1st drop of 2 μL (a,d,g,j,m,p,s,v) after the 2nd drop of 3 μL (b,e,h,k,n,q,t,w), after the 3rd drop of 3 μL (c,f,i,l,o,r,u,x) from the catalytic ink of the JM20 sample using various techniques of the preparation of the catalytic ink: VN1—standard technique by using the 1% Nafion solution (a–f); VM1—1% LF4-SK solution (g–l); VM2—2% LF4-SK solution (m–r); VM0.05—0.05% LF4-SK solution (s–x). Drying options: in air without rotation; in air at a rotation speed of 700 rpm.

For the standard catalytic ink using the 1% Nafion solution (VN) widely described in the literature [11,35], the stationary drying results in the uneven formation of a layer, with the catalyst islands observed despite the three-stage procedure (Figure 4c). The stationary drying in air leads to the formation of a non-uniform catalytic layer on the RDE surface (Figure 4c,o,u). The formation of a thin catalytic layer that is uniform in thickness and structure on the surface of the glass–carbon disk requires the rotation of the RDE. The recommended and frequently used rotation speed in various techniques is 700 rpm. The experiment carried out also shows that the disk rotation at 700 rpm contributes to the formation of a more uniform catalytic layer. For some compositions of the catalytic ink (VM1, VM2) coupled with the drying of the layer during rotation, we have succeeded in obtaining a high-quality catalytic layer completely covering the glass–carbon disk (Figure 4i,r).

For the catalytic layers formed at 700 rpm (Figure 4f,l,r,x), their electrochemical characteristics have been additionally studied (Figure 5). Three characteristic regions can be observed in the CVs of the Pt/C catalyst. In the hydrogen region (0.03–0.3 V), the processes of the formation and desorption of adsorbed hydrogen proceed reversibly. The double-layer region in the CVs corresponds to the charging processes of the double electric layer and

is in the potential range of 0.35–0.7 V. The oxygen region (0.7–1.0 V) is characterized by a significant irreversibility of the processes involving oxygen.

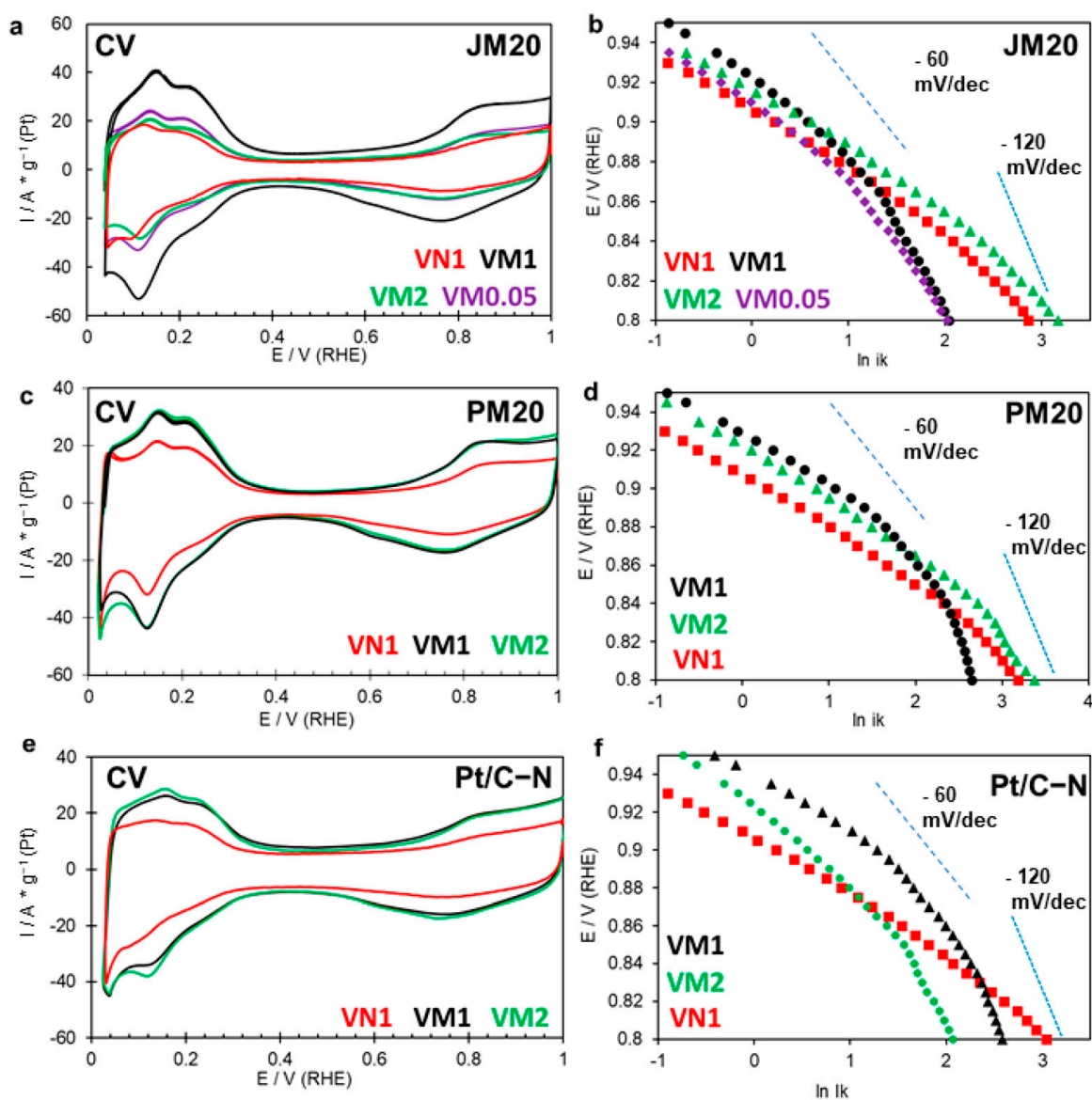


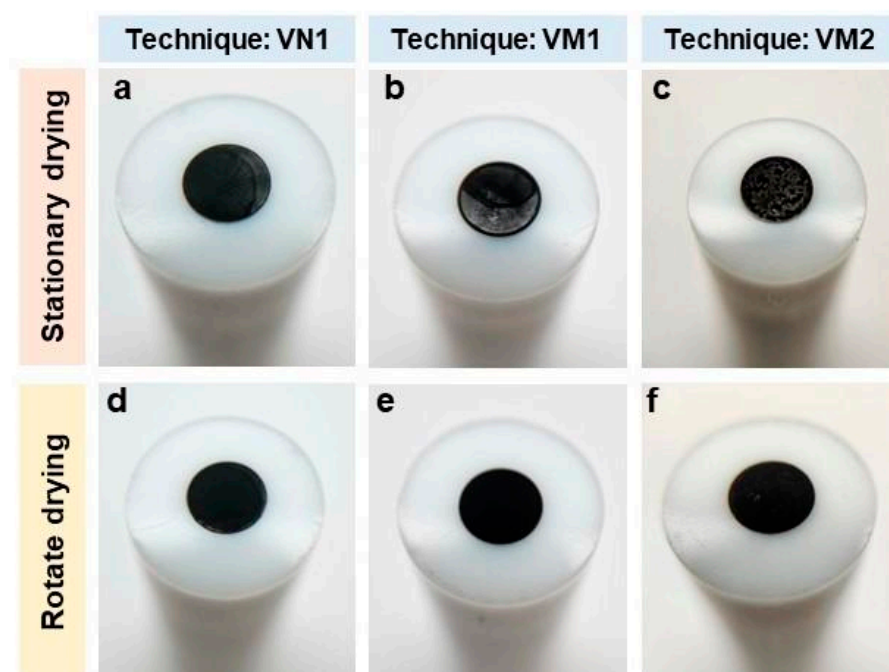
Figure 5. Cyclic voltammograms of the JM20 (a), PM20 (c) and Pt/C–N (e) samples. The potential sweep rate is 20 mV s^{-1} . 2nd cycle. The electrolyte is the 0.1 M HClO_4 solution saturated with Ar at atmospheric pressure. Tafel plots of the ORR: JM20 (b), PM20 (d), Pt/C–N (f). The RDE rotation speed is 1600 rpm . 0.1 M HClO_4 . O_2 atmosphere.

The highest currents in the hydrogen region (Figure 5a) are characteristic of the catalytic layer of the JM20 catalyst prepared using the 1% LF4-SK ionomer (Figure 5a). The ESA values and the ORR mass activity correlate well with the quality of the drop on the RDE surface (Table 2).

It is worth noting that the lowest values of functional characteristics of the JM20 catalyst have been obtained for the island-coated electrodes (Figure 6f,x) prepared by the VM0.05 and VN1 techniques (Table 2). It should also be pointed out that the widespread technique of preparing the ink with 1% Nafion does not result in higher values of the ESA or mass activity.

Table 2. Electrochemical characteristics obtained for various catalytic ink of the PM20, JM20 and Pt/C-N catalysts.

Electrocatalyst	Ink Preparation Technique	ESA, m ² /g (Pt)	ORR Activity	
			I _k , A/g (Pt)	E _{1/2} , V
JM20	VN	74	268	0.89
	VM1	135	384	0.92
	VM2	92	350	0.91
	VM0.05	106	235	0.90
PM20	VN	82	290	0.90
	VM1	96	484	0.93
	VM2	95	455	0.93
Pt/C-N	VN	63	299	0.90
	VM1	103	581	0.93
	VM2	113	326	0.91

**Figure 6.** Photographs of a thin layer at the RDE of the PM20 catalytic ink using various techniques of preparing the catalytic ink: VN (standard technique using the 1% Nafion solution); VM1 (1% LF4-SK solution), VM2 (2% LF4-SK solution). Drying options: drying in air without rotation (a–c); drying in air at 700 rpm (d–f).

The ESA values for the studied JM20 ink grow in the order: VN < VM2 < VM0.05 < VM1 from 74 to 135 m²/g (Pt). The ORR mass activity value increases in the order: VM0.05 < VN < VM2 < VM1 from 235 to 384 A/g (Pt). The increase in the mass activity value during the transition from the 2% to 1% solution of the LF4-SK ionomer is associated with the formation of a more uniform layer on the RDE surface, as well as the absence of oxygen transport difficulties towards the surface of NPs. When using the most diluted 0.05% ionomer solution (VM0.05 technique), we expected to observe an increase in activity due to a decrease in the content of this component in the ink, which is also an insulator for oxygen molecules. The use of the most diluted 0.05% LF4-SK solution has led to a decrease in the ESA and mass activity compared to the 1% solution, despite the absence of any transport difficulties. The decrease in the ORR activity for this ink may be associated with the loss of a part of the catalyst during rotation due to a decrease in the content of the ionomer, which

also acts as a binding component and prevents the detachment of the catalyst particles from the RDE surface [36].

The use of the 1% and 2% LF4-SK solutions as an ionomer in the preparation of the ink of the JM20 electrocatalyst has allowed obtaining a more uniform layer on the RDE surface compared to the other ink preparation techniques. The obtained uniform catalytic layers on the RDE surface demonstrate the increased activity in the ORR (Table 2, Figure S1a). The Tafel slope value observed on carbon-supported Pt catalysts in acid amounts to -60 mV/dec ($-2.3RT/F$) at lower overpotentials and -120 mV/dec ($-2 \times 2.3RT/F$) at higher overpotentials. The experimental data have been fitted to two Tafel slope regions at low ($E > 0.85$ V) and high ($E < 0.85$ V) overpotentials (Figure 5b). It is noteworthy that in the low overpotential region, the Tafel slopes are close when using a different amount of ionomer, whereas in the high overpotential region, for the VM2 and VN1 materials, the Tafel slopes are less negative (Figure 5b).

To further investigate the effect of the ionomer on the electrochemical characteristics of the PM20 and Pt/C–N catalysts, the following techniques have been selected: (i) Standard VN technique; (ii) VM1 technique; and (iii) VM2 technique. The visual quality control of the catalytic layer has been performed after applying the third drop of the ink (stage 3), during the stationary drying, and at a rotation speed of 700 rpm.

According to the results of the study of the PM20 and Pt/C–N catalysts, it has been noted that drying the ink of all the electrocatalysts at a rotation speed of 700 rpm, similar to JM20, allows obtaining a more uniform layer on the RDE surface, at which there are no catalyst islands or coffee rings (Figures 6d–f and 7d–f).

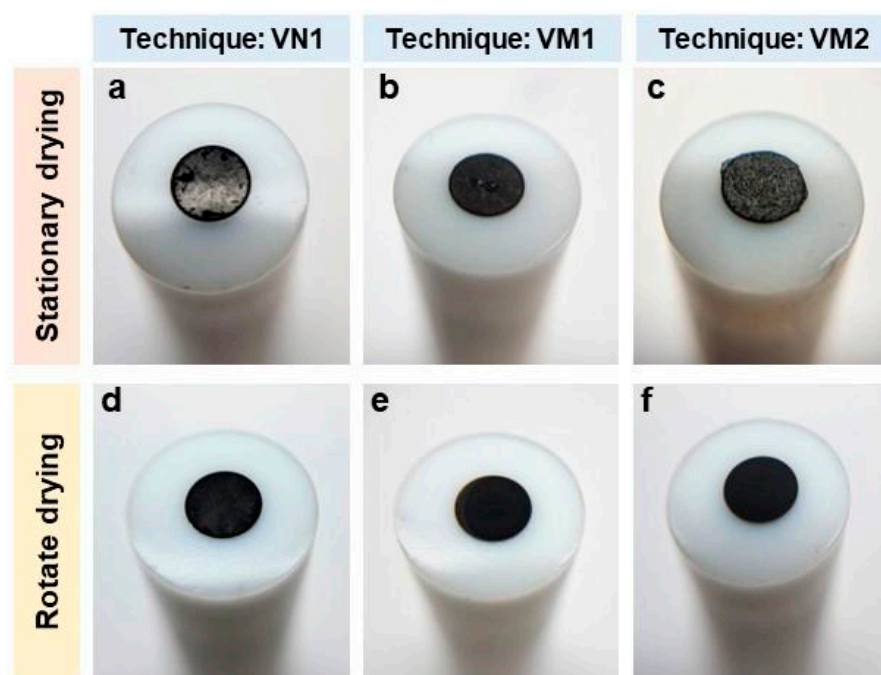


Figure 7. Photographs of a thin layer at the RDE of the Pt/C–N catalytic ink using various techniques of preparing the catalytic ink: VN (standard technique using the 1% Nafion solution); VM1 (1% LF4-SK solution), VM2 (2% LF4-SK solution). Drying options: drying in air without rotation (a–c); drying in air at 700 rpm (d–f).

In the CVs obtained for the PM20 and Pt/C–N catalysts, the highest currents in the hydrogen region are characteristic of the ink prepared according to the VM1 and VM2 techniques using the 1% and 2% LF4-SK solutions as an ionomer (Figure 5c,e). The current value in the hydrogen region at the same double-layer region of the CVs is directly proportional to the value of the ESA, which grows in the order: VN < VM2 < VM1 for both PM20 and Pt/C–N (Table 2). The values of the mass activity and the half-wave potential

differ significantly for the samples studied when using different ink preparation techniques (Figure S1).

The higher ORR activity and $E_{1/2}$ values for the PM20 and Pt/C–N catalysts compared to JM20 (Table 2, Figure S1) are associated with morphological features of the catalysts, including the higher uniformity of the NPs' distribution and a higher proportion of NPs with an average size of less than 2 nm.

The mass activity value for the Pt/C–N catalyst in the ORR calculated from the linear sweep voltammograms (LSVs) recorded at different rotation speeds of the RDE (Figure S1) at a potential of 0.9 V is 1.5 times higher than that for the commercial Pt/C catalyst using the same VM1 technique (Figure S2). The significantly higher activity of the obtained Pt/C–N catalyst compared to JM20 and PM20 can be associated both with the optimal arrangement of platinum NPs due to a decrease in the total number and proportion of micropores in the support and with the positive effect of nitrogen atoms on the spatial distribution and the ORR activity of platinum NPs [33,37–39].

An increase in the mass activity to the values of 484 and 581 A/g(Pt) is characteristic of PM20 (Figure 5d) and Pt/C–N (Figure 5f), respectively, when using the VM1 ink preparation technique with the 1% LF4-SK solution. This technique is considered optimal in terms of obtaining high-quality catalytic layers with enhanced characteristics, regardless of the catalyst used.

3. Materials and Methods

3.1. Research Objects

The following platinum–carbon materials with a 20% platinum loading were selected as electrocatalysts: the commercial materials JM20 (HiSPEC3000, Johnson Matthey, UK) and PM20 (Prometheus R&D LLC, Russia) and the synthesized Pt/C material on an N-doped support Ketjenblack EC-300J.

Preparation of Pt/C–N. The treatment of the carbon support in a mixture with melamine in a ratio of 1:1 was carried out at a temperature of 600 °C in a tube furnace in an argon atmosphere for an hour. A weighed amount of the resulting carbon support (0.15 g) was placed in 18 mL of ethylene glycol ($C_2H_4(OH)_2$) (top grade, 99.8%, Vekton, Russia). The suspension was stirred on a magnetic stirrer (IKA C-MAG HS 7) for 15 min, after which it was placed in an ultrasonic homogenizer (SX-SONIC 1200N1935) for 1 min at an amplitude of 50% and a power of 750 W. Further, with constant stirring, the calculated amount of the platinum hydrochloric acid solution (Pt mass fraction 37.85%, Aurat, Russia) was added with a concentration of 17.9 mg(Pt)/mL and stirred for 5 min, after which 0.5 M NaOH (chemically pure) ($n(OH)/n(Pt) = 12$) was added. The mixture was transferred to a round-bottomed flask with a volume of 100 mL. With constant stirring, 1 mL of formaldehyde was added (top grade, 37.5%, Aquatest, Russia). Next, the temperature was raised to 80 °C in an inert atmosphere, and the reaction mixture was kept with constant stirring for 2 h. After natural cooling of the suspension for 40 min, the product was filtered by repeatedly rinsing the filtrate with portions of isopropyl alcohol and bidistilled water. The catalysts were kept for 1 h in a loss-on-drying oven (SNOL 58/350) at 80 °C and then in a desiccator over P_2O_5 (chemically pure) for 12 h.

LF4-SK (Plastpolymer JSC, St. Petersburg, Russia) and Nafion DE1021 (DuPont, USA) were used as ionomers.

3.2. Composition and Structural-Morphological Characteristics of Materials

Using the transmission electron microscopy (TEM) method, the features of the size and spatial distribution of platinum NPs over the surface of the carbon support were studied. The TEM micrographs were recorded using the JEM-2100 (JEOL, Japan) microscope at a voltage of 200 kV and a resolution of 0.2 nm. The electrocatalyst powders (0.5 mg) were placed in 1 mL of isopropanol to prepare the samples for the TEM analysis. The powder sample was preliminarily dispersed with ultrasound in isopropanol for 10 min. Next, a drop of the resulting suspension was applied with a pipette tip to the copper mesh coated

with a carbon film. The mesh was then placed in a holder installed in the column of the transmission electron microscope. The histograms of the size distribution of platinum NPs in the catalysts were plotted based on the results of determining the sizes of at least 400 randomly selected particles in the TEM micrographs. The average size of NPs (D_{NP}) was determined from the results of plotting the histograms of the size distribution. The accuracy of the D_{NP} determination was $\pm 10\%$.

The average crystallite size (D_{av}) was determined by the X-ray phase analysis. The X-ray patterns were recorded at room temperature using the ARL X'TRA diffractometer (Thermo Fisher Scientific) with filtered $CuK\alpha$ radiation ($\lambda = 0.154056$ nm). The scattering angle was from 15° to 55° 2θ with a detector movement step of 0.02° . The resulting diffraction patterns were processed using the SciDavis software (v.2.7). A Lorentz fit was performed to separate two overlapping platinum peaks (111) and (200), with the required parameters being measured. The error in determining D_{av} was no more than 10%.

3.3. Testing the Technique of Applying the Catalytic Ink onto the RDE

The suspension was prepared according to the previously developed method [40,41] by placing 6 mg of the 20% Pt/C sample in a 10 mL penicillin vial with a mixture of 1.8 mL of isopropyl alcohol (ultra-high purity), 100 mL of deionized water, and 100 mL of the Nafion polymer aqueous emulsion (DE1021) with different mass fraction (Table 3), whereas the I:C ratio varied from 0.1 to 0.4. After the bar was immersed in the suspension, the vial was placed on a magnetic stirrer and stirred for 5 min. Further, the vial was immersed in an ultrasonic bath filled with ice water, and the suspension was homogenized for 10 min at an operating frequency of 35 kHz. After that, the vial was again placed on a magnetic stirrer, and the stirring/ultrasonic treatment procedure was repeated three times.

Table 3. Designation of the catalytic ink obtained using various solutions of ionomers.

Name of the Experiment	Catalyst	Ionomer	Mass Fraction of Ionomer in the Emulsion, %	I:C Ratio	Note
VN	JM20	Nafion	1	0.2	Standard technique
VM1	JM20	LF4-SK	1	0.2	Standard technique with an alternative ionomer
VM2	JM20	LF4-SK	2	0.4	More concentrated ionomer
VM0.05	JM20	LF4-SK	0.05	0.1	Diluted ionomer

As a result, a stable suspension of the catalytic ink was obtained. Next, a layer of the catalytic ink was applied onto the degreased disk electrode, with this layer being formed by threefold application of the aliquots of 2, 3, and 3 μL each (to provide a total platinum loading at the electrode of 20–24 $\mu\text{g}/\text{cm}^2$). At the stage of drying the drops on the RDE surface, the conditions were changed: the drying was conducted in a stationary way (statically), at a disk rotation speed of 300 rpm until the drop dried completely (about 6 min), and at a disk rotation speed of 700 rpm until the drop dried completely (about 5 min).

Using the bipotentiostat Pine AFCBP1 (Pine Research Instruments, USA), a potential sweep was set, and current values were fixed. Initially, to standardize the electrode surface and completely remove any impurities, 100 cycles of potential scanning were carried out at a rate of 200 mV s^{-1} in the range of potentials from 0.04 to 1.00 V (relative to RHE). Then, 2 cyclic voltammograms (CVs) were recorded in the potential range of 0.04–1.00 V at a scanning rate of 20 mV s^{-1} in order to determine the ESA of the catalyst. The amount of electricity was calculated in the “hydrogen” regions of the CVs in the current–time coordinates using the aftermath software. The ESA value was calculated by averaging the amount of electricity spent on the electrochemical adsorption and desorption of atomic hydrogen during the registration of the second cycle using Formula (1):

$$\text{ESA} = ((Q_{ad} + Q_d) \times 0.5) / (210 \times m(\text{Pt}) \times 1000) \quad (1)$$

where ESA is the area of electrochemically active platinum surface ($\text{m}^2 \cdot \text{g}^{-1}$ (Pt)), Q_{ad} and Q_{d} are the charge amounts consumed for the electrochemical adsorption and desorption of atomic hydrogen, respectively (μC), 210 is the charge required for the formation/oxidation of an atomic hydrogen monolayer per 1 cm^2 of platinum surface ($\mu\text{C cm}^{-2}$), and $m(\text{Pt})$ is the platinum weight on the electrode (g). All measurements were performed at room temperature. The accuracy of the ESA determination was $\pm 10\%$.

To evaluate the catalysts' behavior in the ORR, the background potentiodynamic polarization curve was measured in argon at 1600 rpm in the range of potentials from 0.1 to 1.2 V. Further, the electrolyte was saturated with oxygen for an hour, and the potentiodynamic curves were measured at the potential sweep rate of 20 mV s^{-1} in the range from 0.1 to 1.2 V at four disk electrode rotation speeds: 400, 900, 1600, and 2500 rpm.

The following values were chosen as the key parameters for the comparative evaluation of the catalysts' ORR activity: Kinetic current (i_k), mass-related kinetic current (i_{mass}), then ESA-related kinetic current (i_{sp}), and potential value ($E_{1/2}$). The accuracy of the determination was $\pm 10\%$.

To determine the kinetic current, the corresponding graph was plotted in the Koutetsky–Levich coordinates. The current density was determined by the magnitude of the line segment intercepted on the Y-axis. Next, taking into account the geometric area of the disk electrode, the kinetic current value was obtained.

4. Conclusions

The use of PM20 and Pt/C–N electrocatalysts with excellent electrochemical characteristics due to their morphological features is a priority task in the field of hydrogen energy. The selection of a composition of the catalytic ink, in particular the choice of an ionomer, its concentration, and conditions for the formation of a layer on the RDE surface, is a necessary stage for the transition from one technique to another. The study of the catalysts at the RDE is the most essential express assessment of the quality of the electrocatalysts and the catalytic ink obtained on their basis.

The result of optimizing the composition of the catalytic ink and the drying process at the RDE consists of drawing the following conclusions:

1. LF4-SK can be used as an ionomer when preparing the catalytic ink of the platinum–carbon catalysts instead of Nafion.
2. The optimal content of the ionomer for the preparation of the catalytic ink is the I:C ratio – 0.2 of the LF4-SK ionomer.
3. The best way to dry a drop on the RDE surface for all compositions and all types of catalysts is drying at a rotation speed of 700 rpm.

The combination of using the I:C ratio – 0.2 and drying at a rotation speed of 700 rpm makes it possible to obtain the most uniform layer of the catalytic ink and, thus, significantly enhance the electrochemical characteristics of the electrocatalysts in the ORR.

The longer stability tests for the catalytic layer are expected to become the next stage of the study to reasonably replace Nafion with another type of ionomer. Further development of the topic is expected to be associated with the use of the LF4-SK ionomer with the I:C ratio – 0.2 as a binding component in the preparation of the catalytic ink for studies in the MEAs. In this work, we used polymers that had an identical structural unit and differed only in the content of fixed groups. The results obtained are general for polymers with a Nafion-type structure.

Supplementary Materials: The following supporting information can be downloaded at: <https://www.mdpi.com/article/10.3390/inorganics12010023/s1>, Figure S1. LSV curves: JM20 (a), PM20 (b) and Pt/C–N (c). Rotation speed of RDE is 1600 rpm. 0.1 M HClO_4 . Figure S2. Influence ionomer content to ESA value (a) and ORR activity (kinetic current) for different Pt-based catalysts: JM20, PM20 and Pt/C–N.

Author Contributions: Conceptualization, V.G. and A.A.; methodology, S.B.; software, D.M.; validation, E.M., J.B. and D.A.; formal analysis, A.A.; investigation, I.F.; resources, I.P.; data curation, I.P., D.M. and S.B.; writing—original draft preparation, D.M.; writing—review and editing, A.A., S.B. and V.G.; visualization, J.B.; supervision, V.G.; project administration, A.A.; funding acquisition, I.F. All authors have read and agreed to the published version of the manuscript.

Funding: This work was supported by the Russian Science Foundation and Kuban Science Foundation (project No 22-19-20101), <https://rscf.ru/project/22-19-20101/>, accessed on 1 January 2022.

Data Availability Statement: The data presented in this study are available in article/Supplementary Materials.

Acknowledgments: The authors are grateful to Maltsev, A.V. for the support in translation and editing processes and the assistance in communication with the editorial board. The authors are grateful to Nikulin A.Yu. for the assistance in the XRD pattern registration. The authors appreciate the support by LLC “PROMETHEUS R&D” (Rostov-on-Don) and LLC “Systems for Microscopy and Analysis” (Skolkovo, Moscow) for conducting the TEM and EDX studies. The authors are grateful to the Shared Use Center “High-Resolution Transmission Electron Microscopy” (SFedU) for conducting the TEM and EDX studies.

Conflicts of Interest: The authors declare no conflicts of interest.

References

1. Mancino, A.N.; Menale, C.; Vellucci, F.; Pasquali, M.; Bubbico, R. PEM Fuel Cell Applications in Road Transport. *Energies* **2023**, *16*, 6129. [[CrossRef](#)]
2. Zhang, Y.; Wang, J.; Yao, Z. Recent Development of Fuel Cell Core Components and Key Materials: A Review. *Energies* **2023**, *16*, 2099. [[CrossRef](#)]
3. Duan, Y.; Liu, H.; Zhang, W.; Khotseng, L.; Xu, Q.; Su, H. Materials, components, assembly and performance of flexible polymer electrolyte membrane fuel cell: A review. *J. Power Sources* **2023**, *555*, 232369. [[CrossRef](#)]
4. Liu, H.; Ney, L.; Zamel, N.; Li, X. Effect of catalyst ink and formation process on the multiscale structure of catalyst layers in PEM fuel cells. *Appl. Sci.* **2023**, *12*, 3776. [[CrossRef](#)]
5. Ngo, T.T.; Yu, T.L.; Lin, H.L. Nafion-based membrane electrode assemblies prepared from catalyst inks containing alcohol/water solvent mixtures. *J. Power Sources* **2013**, *238*, 1–10. [[CrossRef](#)]
6. Jinnouchi, R.; Kudo, K.; Kodama, K.; Kitano, N.; Suzuki, T.; Minami, S.; Shinozaki, K.; Hasegawa, N.; Shinohara, A. The role of oxygen-permeable ionomer for polymer electrolyte fuel cells. *Nat. Commun.* **2023**, *12*, 4956. [[CrossRef](#)]
7. Welch, C.; Labouriau, A.; Hjelm, R.; Orlor, B.; Johnston, C.; Kim, Y.S. Nafion in dilute solvent systems: Dispersion or solution? *ACS Macro Lett.* **2012**, *1*, 1403–1407. [[CrossRef](#)]
8. Dixit, M.B.; Harkey, B.A.; Shen, F.; Hatzell, K.B. Catalyst layer ink interactions that affect coatability. *J. Electrochem. Soc.* **2018**, *165*, F264–F271. [[CrossRef](#)]
9. Passalacqua, E.; Lufrano, F.; Squadrito, G.; Patti, A.; Giorgi, L. Nafion content in the catalyst layer of polymer electrolyte fuel cells: Effects on structure and performance. *Electrochim. Acta* **2001**, *46*, 799–805. [[CrossRef](#)]
10. Ishikawa, H.; Sugawara, Y.; Inoue, G.; Kawase, M. Effects of Pt and ionomer ratios on the structure of catalyst layer: A theoretical model for polymer electrolyte fuel cells. *J. Power Sources* **2018**, *374*, 196–204. [[CrossRef](#)]
11. Shinozaki, K.; Zack, J.W.; Pylypenko, S.; Pivovar, B.S.; Kocha, S.S. Oxygen reduction reaction measurements on platinum electrocatalysts utilizing rotating disk electrode technique: II. Influence of ink formulation, catalyst layer uniformity and thickness. *J. Electrochem. Soc.* **2015**, *162*, F1384. [[CrossRef](#)]
12. Harada, M.; Kajiya, S.; Mitsuoka, T.; Takata, S.I.; Iwase, H.; Aoki, H. Scattering investigations into the structures of polymer-electrolyte-fuel-cell catalyst layers exhibiting robust performance against varying water fractions of catalyst ink solvents. *Colloids Surf. A Physicochem. Eng. Asp.* **2023**, *665*, 131183. [[CrossRef](#)]
13. Singh, R.K.; Devivaraprasad, R.; Kar, T.; Chakraborty, A.; Neergat, M. Electrochemical impedance spectroscopy of oxygen reduction reaction (ORR) in a rotating disk electrode configuration: Effect of ionomer content and carbon-support. *J. Electrochem. Soc.* **2015**, *162*, F489. [[CrossRef](#)]
14. Holdcroft, S. Fuel cell catalyst layers: A polymer science perspective. *Chem. Mater.* **2014**, *26*, 381–393. [[CrossRef](#)]
15. Kocha, S.S.; Zack, J.W.; Alia, S.M.; Neyerlin, K.C.; Pivovar, B.S. Influence of ink composition on the electrochemical properties of Pt/C electrocatalysts. *ECS Trans.* **2013**, *50*, 1475. [[CrossRef](#)]
16. Singh, S.; Grabowski, J.P.; Pohani, S.; Apuzzo, C.F.; Platt, D.C.; Jones, M.A.; Mitchell, T.A. Synthesis of Polycyclic Ether-Benzopyrans and In Vitro Inhibitory Activity against *Leishmania tarentolae*. *Molecules* **2020**, *25*, 5461. [[CrossRef](#)]
17. Nesselberger, M.; Ashton, S.; Meier, J.C.; Katsounaros, I.; Mayrhofer, K.J.; Arenz, M. The particle size effect on the oxygen reduction reaction activity of Pt catalysts: Influence of electrolyte and relation to single crystal models. *J. Am. Chem. Soc.* **2011**, *133*, 17428–17433. [[CrossRef](#)]

18. Ke, K.; Hiroshima, K.; Kamitaka, Y.; Hatanaka, T.; Morimoto, Y. An accurate evaluation for the activity of nano-sized electrocatalysts by a thin-film rotating disk electrode: Oxygen reduction on Pt/C. *Electrochim. Acta* **2012**, *72*, 120–128. [CrossRef]
19. Garsany, Y.; Baturina, O.A.; Swider-Lyons, K.E.; Kocha, S.S. Experimental Methods for Quantifying the Activity of Platinum Electrocatalysts for the Oxygen Reduction Reaction. *Anal. Chem.* **2010**, *82*, 6321–6328. [CrossRef]
20. Mo, S.; Du, L.; Huang, Z.; Chen, J.; Zhou, Y.; Wu, P.; Meng, L.; Wang, N.; Xing, L.; Zhao, M.; et al. Recent Advances on PEM Fuel Cells: From Key Materials to Membrane Electrode Assembly. *Electrochem. Energy Rev.* **2023**, *6*, 28. [CrossRef]
21. Andersen, S.M.; Grahl-Madsen, L. Interface contribution to the electrode performance of proton exchange membrane fuel cells—Impact of the ionomer. *Int. J. Hydrogen Energy* **2016**, *41*, 1892–1901. [CrossRef]
22. Yakovlev, Y.V.; Lobko, Y.V.; Vorokhta, M.; Nováková, J.; Mazur, M.; Matolínová, I.; Matolín, V. Ionomer content effect on charge and gas transport in the cathode catalyst layer of proton-exchange membrane fuel cells. *J. Power Sources* **2021**, *490*, 229531. [CrossRef]
23. Ahn, C.Y.; Cheon, J.Y.; Joo, S.H.; Kim, J. Effects of ionomer content on Pt catalyst/ordered mesoporous carbon support in polymer electrolyte membrane fuel cells. *J. Power Sources* **2013**, *222*, 477–482. [CrossRef]
24. Zhao, J.; Sarkar, A.; Manthiram, A. Synthesis and characterization of Pd-Ni nanoalloy electrocatalysts for oxygen reduction reaction in fuel cells. *Electrochim. Acta* **2010**, *55*, 1756–1765. [CrossRef]
25. Yaroslavtsev, A.B. Perfluorinated ion exchange membranes. *High Mol. Weight. Compd.* **2013**, *55*, 1367. [CrossRef]
26. Rikukawa, M.; Sanui, K. Proton-conducting polymer electrolyte membranes based on hydrocarbon polymers. *Prog. Polym. Sci.* **2000**, *25*, 1463–1502. [CrossRef]
27. Pure Aqua, Inc. Available online: <https://pureaqua.com/dow-filmtec-membranes/> (accessed on 18 October 2023).
28. Panshin, Y.A.; Dreyman, N.A.; Andreeva, A.I.; Manechkina, O.N. Properties of perfluorinated sulfonic cation exchange membranes MF-4SK. *Plastics* **1977**, *8*, 7–8.
29. Branco, C.M.; El-Kharouf, A.; Du, S. Materials for polymer electrolyte membrane fuel cells (PEMFCs): Electrolyte membrane, gas diffusion layers, and bipolar plates. In *Reference Module in Materials Science and Materials Engineering*; Elsevier: Oxford, UK, 2017; pp. 1–11.
30. Timashev, S.F. *Physico-Chemistry of Membrane Processes*; Chemistry: Moscow, Russia, 1988; 240p.
31. Huy, H.A.; Van Man, T.; Tai, H.T. Preparation and characterization of high-dispersed Pt/C nano-electrocatalysts for fuel cell applications. *Vietnam. J. Sci. Technol.* **2016**, *54*, 472–482. [CrossRef]
32. Paperzh, K.O.; Alekseenko, A.A.; Volochaev, V.A.; Pankov, I.V.; Safronenko, O.A.; Guterman, V.E. Stability and activity of platinum nanoparticles in the oxygen electroreduction reaction: Is size or uniformity of primary importance? *Beilstein J. Nanotechnol.* **2021**, *12*, 593–606. [CrossRef] [PubMed]
33. Moguchikh, E.A.; Paperzh, K.O.; Alekseenko, A.A.; Gribov, E.N.; Tabachkova, N.Y.; Maltseva, N.V.; Tkachev, A.G.; Neskromnaya, E.A.; Melezhik, A.V.; Butova, V.V.; et al. Platinum nanoparticles supported on nitrogen-doped carbons as electrocatalysts for oxygen reduction reaction. *J. Appl. Electrochem.* **2022**, *52*, 231–246. [CrossRef]
34. Liu, G.; McLaughlin, D.; Thiele, S.; Van Pham, C. Correlating catalyst ink design and catalyst layer fabrication with electrochemical CO₂ reduction performance. *Chem. Eng. J.* **2023**, *460*, 141757. [CrossRef]
35. Shinozaki, K.; Zack, J.W.; Pylypenko, S.; Richards, R.M.; Pivovar, B.S.; Kocha, S.S. Benchmarking the oxygen reduction reaction activity of Pt-based catalysts using standardized rotating disk electrode methods. *Int. J. Hydrogen Energy* **2015**, *40*, 16820–16830. [CrossRef]
36. Li, G.F.; Yang, D.; Abel Chuang, P.Y. Defining nafion ionomer roles for enhancing alkaline oxygen evolution electrocatalysis. *ACS Catal.* **2018**, *8*, 11688–11698. [CrossRef]
37. Alekseenko, A.; Pavlets, A.; Moguchikh, E.; Tolstunov, M.; Gribov, E.; Belenov, S.; Guterman, V. Platinum-Containing Nanoparticles on N-Doped Carbon Supports as an Advanced Electrocatalyst for the Oxygen Reduction Reaction. *Catalysts* **2022**, *12*, 414. [CrossRef]
38. Wang, M.; Li, Y.; Han, J. Mesoporous N-doped carbon nanofibers with surface nanocavities for enhanced catalytic activity toward oxygen reduction reaction. *J. Mater. Sci.* **2020**, *55*, 11177–11187. [CrossRef]
39. Zhou, Y.; Neyerlin, K.; Olson, T.S.; Pylypenko, S.; Bult, J.; Dinh, H.N.; Gennett, T.; Shao, Z.; O’Hayre, R. Enhancement of Pt and Pt-alloy fuel cell catalyst activity and durability via nitrogen-modified carbon supports. *Energy Environ. Sci.* **2010**, *3*, 1437–1446. [CrossRef]
40. Paperzh, K.O.; Pavlets, A.S.; Alekseenko, A.A.; Pankov, I.V.; Guterman, V.E. The integrated study of the morphology and the electrochemical behavior of Pt-based ORR electrocatalysts during the stress testing. *Int. J. Hydrogen Energy* **2023**, *48*, 22401–22414. [CrossRef]
41. Paperzh, K.; Alekseenko, A.; Safronenko, O.; Nikulin, A.; Pankov, I.; Guterman, V. UV radiation effect on the microstructure and performance of electrocatalysts based on small Pt nanoparticles synthesized in the liquid phase. *Colloid Interface Sci. Commun.* **2021**, *45*, 100517. [CrossRef]

Disclaimer/Publisher’s Note: The statements, opinions and data contained in all publications are solely those of the individual author(s) and contributor(s) and not of MDPI and/or the editor(s). MDPI and/or the editor(s) disclaim responsibility for any injury to people or property resulting from any ideas, methods, instructions or products referred to in the content.